

MACHINE DIRECTION REGISTRATION DYNAMICS MODEL OF A ROTARY PRINTING PRESS

By

Brian S. Rice¹ and Robert L. Walton
¹Rochester Institute of Technology
USA

ABSTRACT

We derive an analytical model of the machine direction registration dynamics of a continuous-web, electronic line shaft (ELS) rotary printing press. We use the model to quantify the affect of tension disturbances on machine direction registration dynamics with different control schemes. With standard ELS registration control schemes, we show the benefits of using a compensator roller vs. electronic differential gear (advance or retard print cylinder's angular position). Next, we develop a novel cascaded reference control scheme for an electronic differential gear controlled ELS printing press that allows it to rival the performance of a compensator roller controlled ELS printing press. Finally, we demonstrate the benefits of using a cascaded reference empirically on a 6-station rotogravure ELS printing press.

NOMENCLATURE

E	Young's modulus of web
g_{ratio}	gear ratio
h	web thickness
i	motor current
IC	initial condition
J	angular inertia
k_{shaft}	shaft rotational stiffness
K_{dth}	motor back emf constant
K_{ps}	velocity loop proportional gain
K_{is}	velocity loop integral gain
K_{pi}	current loop proportional gain
K_{ii}	current loop integral gain

K_{tqm}	motor torque constant
l	armature inductance
L	web span length
MOP	correction speed
r	armature resistance
R	roller radius
R_{avg}	average roller radius of all ELS cylinders
t	time
T	web span tension
V	motor voltage
V_{CR}	compensator roller speed
V_{DG}	differential gear correction speed
w	web width
x	web length
X	registration error (e.g., X_{35} refers to a registration error between images printed at stations 3 and 5)
X_{CR}	compensator roller position
X_{DG}	differential position difference
ε	web span strain
φ	dummy time index
τ	shaft torque
θ	angular position
$\dot{\theta}$	angular velocity
$\ddot{\theta}$	angular acceleration

Subscript

i	index variable referring to span or roller number
$error$	difference between the addition of reference and trim with feedback
m	motor
p	proportional gain
ref	reference
$trim$	trim to reference value

Superscript

T	transient solution
$delay$	transport delay in variable
ref	reference variable
SS	steady-state solution
$trim$	trim variable based on output of differential gear registration control loop
0	untensioned web

INTRODUCTION

Commercial printing is a huge and rapidly changing industry. The U.S. market alone is estimated to exceed \$140 billion dollars annually [1]. Products made on continuous-web rotary printing presses represent a significant portion of this market. The printing industry is extremely competitive with constant pressure to reduce unit-manufacturing costs. Good color-to-color registration is key to product quality. Registration control is also key in the manufacture of flexible displays and electronics in a roll-to-roll fashion [2].

Figure 1 depicts a 6-station rotary printing press. Registration refers to the ability to lay images down from different printing cylinders onto a web in a known position with respect to each other. Automatic registration control requires a sensor to detect registration marks.

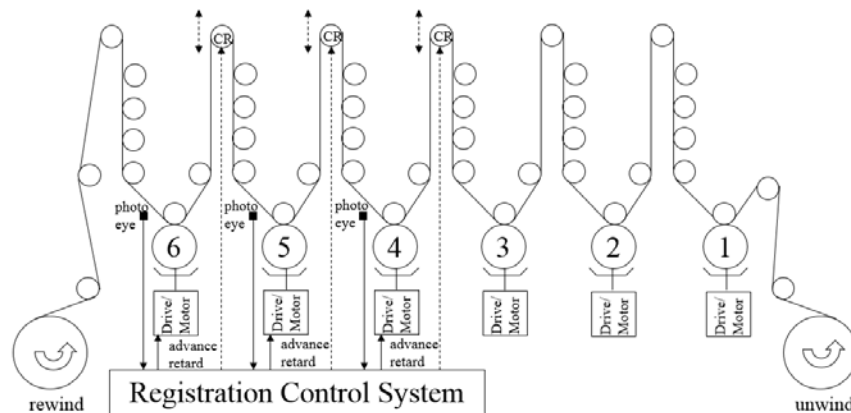


Figure 1 – Schematic of a 6-Station Electronic Line Shaft Printing Press

Let us assume that we desire to print an array of “+” directly on top of an array of “•” in the printing press depicted in Figure 1. A printed image with a lateral and longitudinal translational registration error is shown in Figure 2. We will limit our discussion to longitudinal registration errors only.

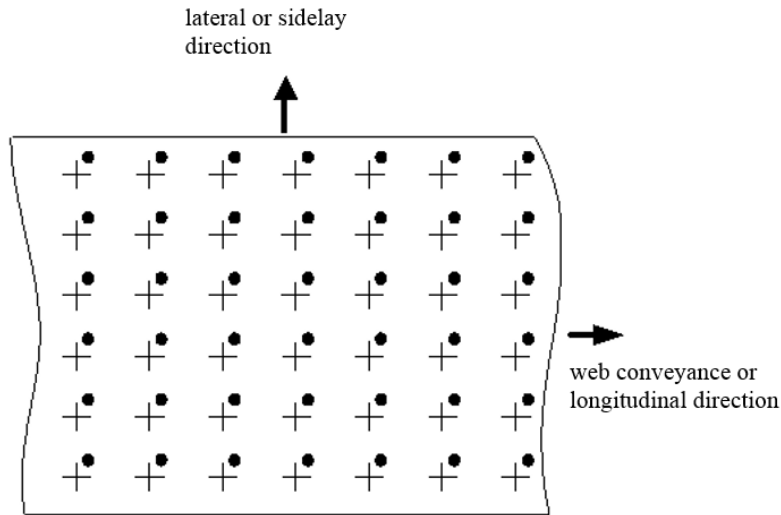


Figure 2 – Schematic of a 6-Station Electronic Line Shaft Printing Press

There are numerous press designs used in the industry. Rotogravure, flexography, letterpress, lithography, screen printing, and digital [1] are common printing methods used on rotary presses. Printing presses have either an electronic line shaft (ELS), typically used in new presses, or a mechanical line shaft (MLS). Compensator rollers (CR) or differential gearing are used to control longitudinal registration for MLS printing presses. Differential gearing refers to changing the relative angular position between printing cylinders mechanically. Compensator rollers (CR) or electronic differential gear (DG) are used to control longitudinal registration for ELS printing presses. DG refers to changing the relative angular position between printing cylinders electronically.

There are two basic modes of active registration control that we term key-color and color-to-color, respectively. We use the 6-station press depicted in Figure 1 to describe the two control methods. In key-color registration, registration errors for each station are referenced back to one “key” station. For example, registration marks printed at stations 4, 5, and 6 are all referenced to marks printed at station 3 for error calculations. In color-to-color registration, each color is compared to the previous color for registration errors. For example, registration marks printed at station 4 are referenced to marks printed at station 3; registration marks printed at station 5 are referenced to marks printed at station 4; and registration marks printed at station 6 are referenced to marks printed at station 5.

The purpose of this paper is study the longitudinal registration dynamics for a typical 6-station ELS rotogravure printing press both analytically and empirically. The analytical equations developed will be general enough to handle any combination of the aforementioned designs. Numerous references [3-8] discuss issues affecting registration control performance. Puckhaber [4] categorizes 65 possible reasons for machine direction registration problems into eight categories. Using a system model, we study how two of these categories—tension variations and registration compensation system—affect registration. We use this model to study the registration response of existing control schemes and a novel control scheme to an infeed tension disturbance. Finally, we demonstrate the benefits of using a cascaded reference empirically on a 6-station rotogravure printing press with DG control.

ANALYTICAL EQUATIONS LONGITUDINAL REGISTRATION DYNAMICS

Figure 3 represents a simple three-span two-station printing press. Equation {1} is the governing equation for longitudinal registration dynamics and is derived in Appendix. This equation builds on the previous work of Brandenburg et al [8-10], Seshadri et al [11], and Kang et al [12].

$$\frac{d}{dt}(X_{21}) = \left(\frac{\dot{\theta}_2 R_2}{1 + \varepsilon_2} - \frac{\dot{\theta}_1^{delay} R_1}{1 + \varepsilon_1^{delay}} \right) + \left(\dot{\theta}_1^{delay} - \dot{\theta}_2 \right) \cdot \frac{R_2 + R_1}{2}. \quad \{1\}$$

This expression may be integrated with respect to time to compute the total registration error in the untensioned web. The “delay” superscript represents the transport delay from stations 1 to 2—the same piece of web is printed at two different stations at different points in time. Equation {2} is the governing equation for longitudinal tension dynamics and was derived by Walton and Rice [13]. This equation advanced the previous work of Brandenburg [8], Young et al [14,15], and Shin [16].

$$L_2 \cdot \frac{d}{dt}(\varepsilon_2) = \left(\frac{\dot{\theta}_2 R_2}{1 + \varepsilon_2} - \frac{\dot{\theta}_1 R_1}{1 + \varepsilon_1} \right) \cdot (1 + \varepsilon_2)^2. \quad \{2\}$$

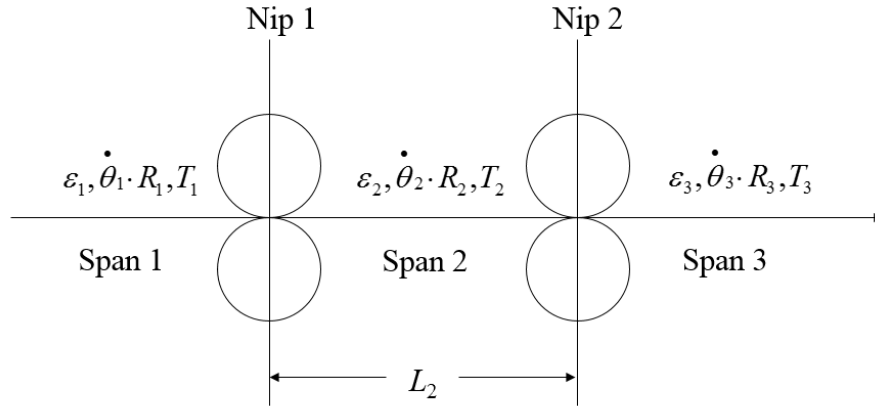


Figure 3 – Simple Two-Roller Conveyance Path

System Model Six-Station Rotogravure Printing Press

We extend the methodology developed in Appendix for the longitudinal registration dynamics of a 2-station MLS printing press to a 6-station ELS printing press depicted in Figure 1. In order to accurately model an ELS press, we need to bring in the dynamics of the velocity and current loops. These dynamics are critical to modeling the response and interactions of the individual drives in an ELS printing press.

Typical registration control loop. A schematic of a typical registration control loop is shown in Figure 4. There is one control loop per station that requires automatic registration, three in our example. Most commercial registration systems use an optical sensor to detect a mark (trapezoid in our example) that is printed once per cylinder

revolution. The sensor looks at the trapezoid marks once every given number of revolutions (Num_Rev). For example, if $Num_Rev = 3$ the registration control loop only updates every three cylinder revolutions. The sensor computes the distance between the trapezoid just printed and a trapezoid printed at an earlier station. This distance is subtracted from the desired distance, 20 mm in our example, yielding the registration error (Reg_Err). If the registration error is smaller than the dead band ($Dead_Band$), it is set equal to zero. If it is larger than maximum correction (Max_Corr), it is set equal to the maximum correction value. Finally, an advance or retard signal is sent out to the registration compensation mechanism that modifies the web length between a pair of cylinders or the surface velocity of a cylinder for a certain length of time. This length of time is equal to Reg_Err divided by the motor-operated pot (MOP) correction speed. After Num_Rev cylinder revolutions, the process described above is repeated. The previous correction does not have to complete prior to a new Reg_Err being computed. (A level of detail beyond what is described here is not typically shared by vendors.)

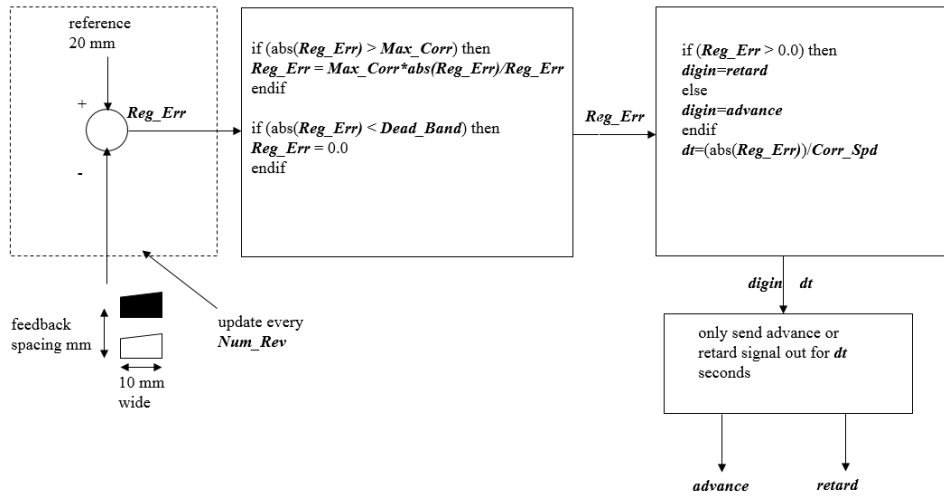


Figure 4 – Schematic of a Typical Registration Control Loop

Typical velocity and current control loops. A schematic of a typical velocity and current control loop for an DG ELS press is shown in Figure 5. For an DG ELS press, the angular velocity reference is trimmed by the MOP rate correction speed for each station that needs to be registered. For a CR ELS machine $spd_trim = 0$, and the MOP correction speed (divided by 2) is used to translate the CR mechanism. The speed-loop control logic is the same for all stations:

$$\dot{\theta}_{error} = \dot{\theta}_{trim} + \dot{\theta}_{ref} - \frac{\dot{\theta}_m}{g_{ratio}}, \quad \{3\}$$

$$i_{ref} = K_{ps} \cdot \dot{\theta}_{error} + K_{is} \cdot \int_0^t \dot{\theta}_{error} d\varphi. \quad \{4\}$$

The current loop control logic is:

$$i_{error} = i_{ref} - i_m, \quad \{5\}$$

$$V = K_{pi} \cdot i_{error} + \int_0^t K_{ii} \cdot i_{error} d\varphi. \quad \{6\}$$

(A level of detail in these control loops beyond what is described here is not typically shared by vendors with ELS systems.) A simple model of an armature-controlled motor [17] is:

$$\frac{d}{dt} i_m = \frac{\left(V - K_{dth} \cdot \dot{\theta}_m - r_m \cdot i_m \right)}{l_m}, \quad \{7\}$$

$$i_m = \int_0^t \frac{d}{d\varphi} (i_m) \cdot d\varphi + IC, \quad \{8\}$$

$$\tau_m = K_{iqm} \cdot i_m. \quad \{9\}$$

For a 6-station press, there will be six sets of the above equations, one for each station.

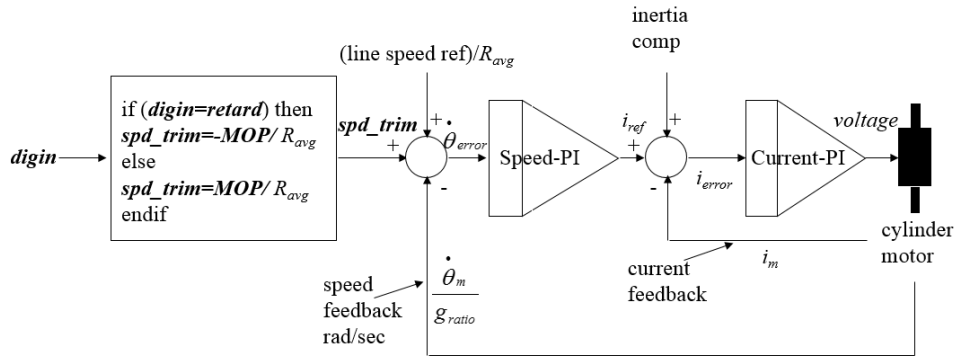


Figure 5 – Schematic of a Typical Velocity Control Loop with an ELS

NUMERICAL EXAMPLES

In this section, we will study how an infeed-tension disturbance affects the registration performance of the printing press depicted in Figure 1. As mentioned in the introduction section, there are two basic modes of active registration control, key-color and color-to-color, and two different control mechanisms, CR or DG. In addition, a new control method, termed “cascade,” will be modeled. The cascade control scheme addresses the deficiency in DG color-to-color control, namely, changing the speed of a print cylinder to correct a registration error introduces a registration error in the subsequent station. For example, changing the speed of the cylinder in station 4 to correct a registration error between stations 3 and 4 introduces a registration error between stations 4 and 5.

A cascaded control scheme addresses this deficiency by “cascading” the speed correction of an upstream cylinder to all downstream cylinders. For example, a speed correction to station 4, based on a registration error between stations 3 and 4, is cascaded to stations 5 and 6. Likewise, a speed correction to station 5, based on a registration error between stations 4 and 5, is cascaded to station 6.

Using the modeling techniques developed in this paper we create a numerical model of a 6-station rotogravure printing press. A schematic of the model with a numbering scheme is shown in Figure 6. We use ACSL™, a commercial ODE solver, to model the examples in this section. We use a second-order Runge-Kutta numerical integration routine with a fixed time of 0.0001 sec.

In the following examples, web speed is 3.75 m/sec, inlet tension T_1 is 99.68 N, web thickness is 4.5 μm , web width is 1.6 m, and coupling stiffness is $4.3 \times 10^6 \text{ N/rad}$. The gravure cylinder radius for all stations, except station 1, is 0.255 m. The radius for station 1 is 35 μm less than the others. (The exact radii for the different stations are not known. A slightly smaller radius is assumed for station 1 based on the actual tension profile discussed in the empirical example section. The smaller radius accounts for a 4.45 N increase in tension from station 1 to station 2.) Young’s modulus of the web is $6.6 \times 10^6 \text{ kPa}$ in the infeed section (21.1 °C) and $4.5 \times 10^6 \text{ kPa}$ in the dryer sections (88 °C). (The values for Young’s moduli were measured from samples of comparable material coated in the experiments for this paper.)

Registration tuning parameters of interest are $Corr_Spd = 0.75 \text{ mm/sec}$, $Num_Rev = 2$, and $Max_Corr = 1.3 \text{ mm}$. The velocity and current loop bandwidths are 20 and 350 rad/sec, respectively. (Bandwidths are computed using Bode diagram techniques. The bandwidths are based on a reduction in transfer function of 0.707 from its steady-state value at low frequency. The transfer function for the velocity loop is the roller angular velocity divided by the speed reference. The transfer function for the current loop is motor torque divided by current reference.)

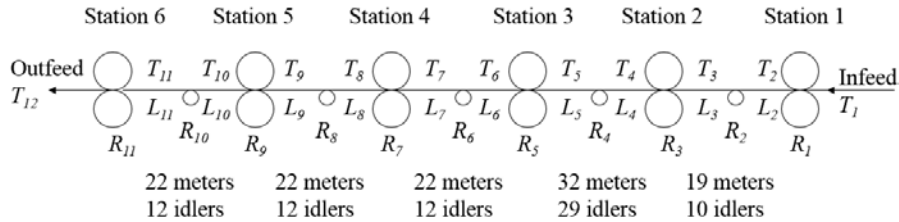


Figure 6 – Schematic of a 6-Station ELS Printing Press Registration Model

Figure 7 shows how a 22.5 N step in the infeed tension (T_1) affects the dryer tensions; the infeed tension step occurs at $t = 10 \text{ sec}$. The control scheme used for this example is DG color-to-color. Tension in the dryer sections reduces by the same percentage, 32%, as the magnitude of Young’s modulus decreases with temperature. Thus, a 22.5 N infeed tension step only results in a 15.3 N increase in the dryers’ steady-state tensions. The bounce in dryer tensions T_9 and T_{11} is a result of the registration controls modifying the last two print cylinders’ speeds in an effort to hold registration.

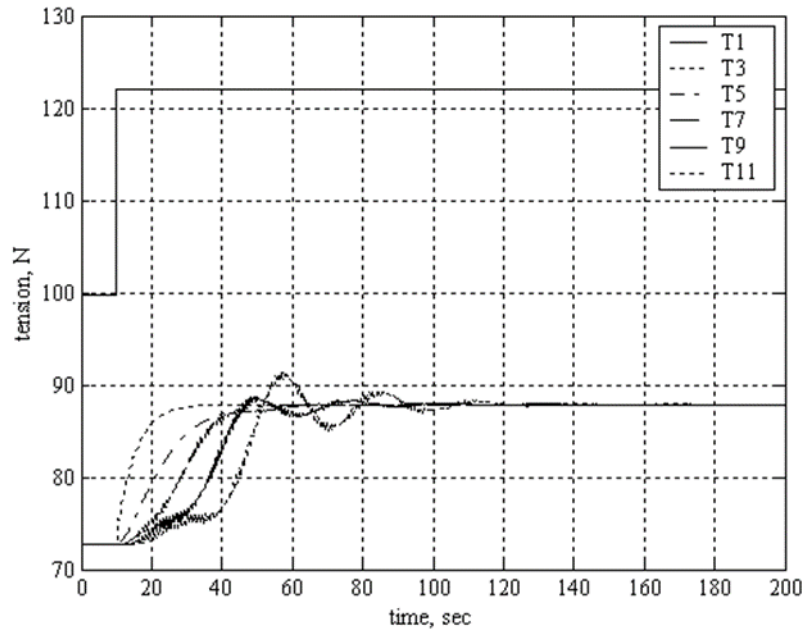


Figure 7 – Dryer Tension Response to an Infeed Tension Step of 22.5 N

Registration performance as a result of the same infeed tension step is shown in Figs. 8 and 9. These figures plot registration error vs. time. Most ELS printing presses today use DG with either a color-to-color or key-color registration control scheme. Figure 8 is a plot of the color-to-color registration errors (X_{34} , X_{45} , X_{56}) for four different control schemes. Here, color-to-color refers to the registration error not the control scheme. Figure 9 is a plot of the key-color registration errors (X_{34} , X_{35} , X_{36}) for the same control schemes as shown in Figure 8. Here, key-color refers to the registration error not the control scheme. Very little difference between DG with color-to-color or key-color control is seen in either Figs. 8 or 9; here, color-to-color is referring to the control scheme.

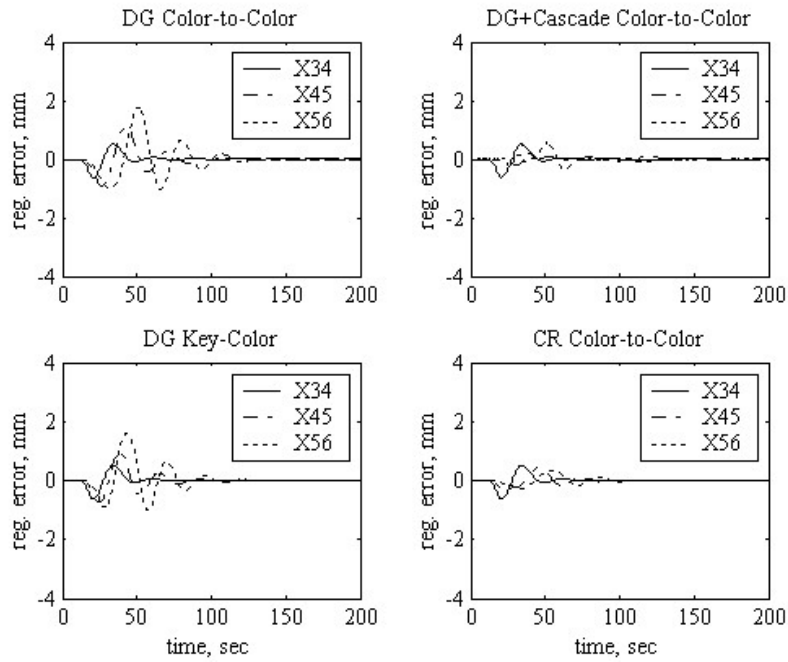


Figure 8 – Color-to-Color Registration Error

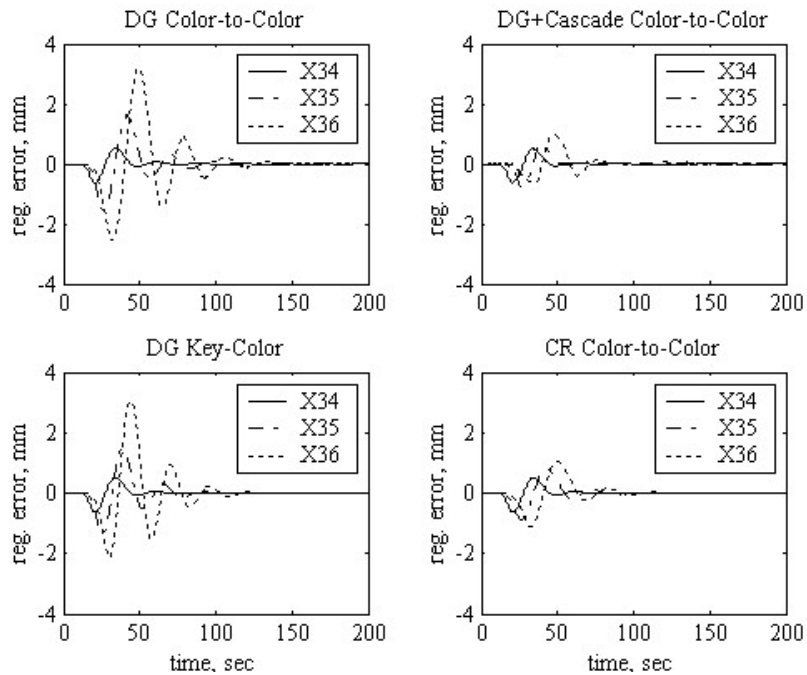


Figure 9 – Key-Color Registration Error

The peak-to-valley registration error X_{56} is 2.8 mm with DG color-to-color control. One method to improve registration performance is to use a CR with color-to-color control. With CR control, the peak-to-valley registration error X_{56} is 0.7 mm. While CR control significantly improves registration performance over DG, CR control has the obvious disadvantage of additional hardware. Using the model a new control method termed DG cascaded color-to-color control is investigated. DG with a cascaded color-to-color control scheme has a peak-to-valley registration error X_{56} of 0.9 mm. This new control method has essentially same registration performance improvement as the CR color-to-color method. (The same registration, velocity, and current loop-control gains were used to model the different registration control schemes. The controller gains were optimized for the base case DG color-to-color only. No attempt was made to re-optimize them for the other control schemes.)

COMPARISON OF NUMERICAL AND EMPIRICAL RESULTS

In this section, we compare the model-predicted response with empirical data from an ELS printing press using DG color-to-color control and DG with cascaded color-to-color control, respectively. The disturbance is the same 22.5 N infeed tension step studied in the previous section. Figures 10 and 11 show a comparison of model data with actual data from the 6-station gravure printing press with an DG using standard color-to-color registration control. Figure 11 shows a comparison of our model with an actual 6-station gravure printing press with an ELS DG using cascaded color-to-color registration control. Table 1 shows a comparison of peak-to-valley registration errors for the two control schemes of interest for both actual and model data.

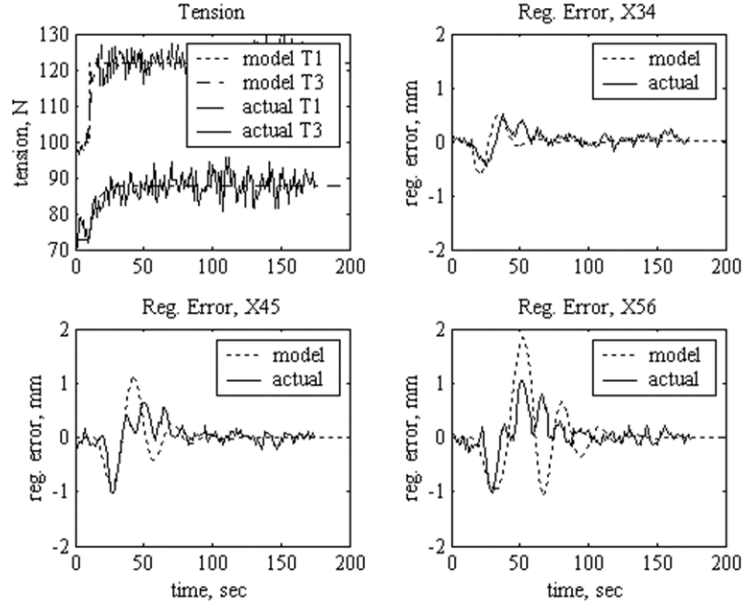


Figure 10 – ELS DG Color-to-Color Registration Control, Model vs. Empirical

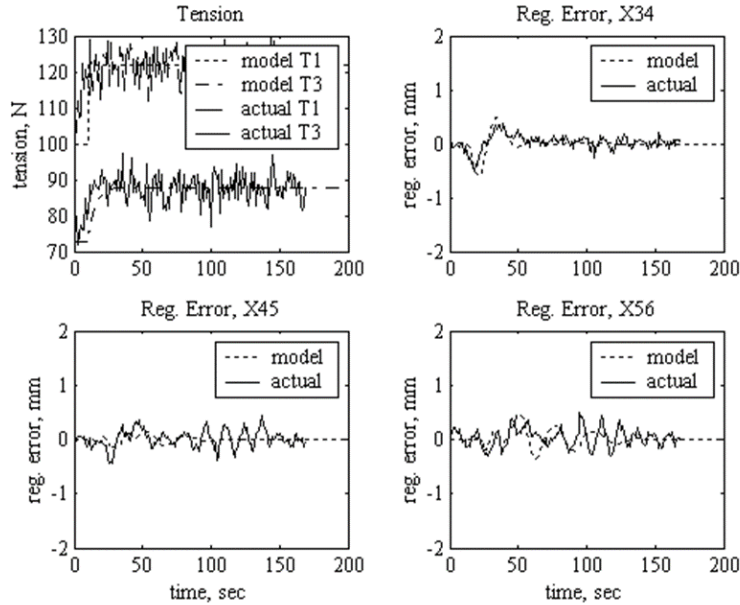


Figure 11 – ELS DG Cascade Color-to-Color Registration Control, Model vs. Empirical

Reg. Error (mm)	DG Color-to-Color		DG Cascade Color-to-Color	
	Model	Actual	Model	Actual
X_{34}	1.1	1.0	1.1	0.9
X_{45}	2.1	1.7	0.4	0.9
X_{56}	2.8	2.1	0.9	0.8

Table 1 – Comparison of Model to Actual Peak-to-Valley Registration Errors

As evidenced by Figs. 10 and 11 and Table 1, correlation between model and actual tension and registration data is excellent. Both actual and model data show the cascaded control scheme significantly reduces the peak-to-valley registration errors X_{45} and X_{56} vs. the standard DG control method. Both the actual and model data show a reduction in X_{56} registration error by a factor of 0.3 and 0.4, respectively.

(Actual data has additional fluctuations—higher frequency—that the model does not contain. This is likely due to sources of noise that are not accounted for in the model. Noise sources include: doctor blade oscillation, nonuniform cylinder-frictional properties, which is due to the presence of liquid being only present in the etched areas of the cylinder, dryer pressure fluctuations, roller imbalance, roller run-out, etc.).

SUMMARY

We derived an analytical model of the machine direction registration dynamics of a continuous web ELS, 6-station rotary printing press. With standard registration control schemes, we showed the benefits of using CR vs. DG. A novel, cascaded reference control scheme for an DG ELS printing press was developed. It allowed an DG-

controlled press to rival the performance of a CR-controlled press. Actual data from an ELS press was used to verify our model and show the benefits of our new cascaded-control, registration-control scheme for DG ELS presses.

ACKNOWLEDGMENTS

We thank Reto Keller, Rockwell Automation AG Switzerland, for his exceptional AutoMax® programming skills. We thank Douglas Newton, Eastman Kodak Co. USA, for allowing us to implement an experimental control scheme during commissioning of a production printing press.

REFERENCES

1. “Gravure Education Foundation and Gravure Association of America,” Gravure Process and Technology, Rochester, NY, 2003.
2. Fuchigami, S., “Challenges and Opportunities in Flat Panel Industry,” Proceedings of the Eight International Conference on Web Handling, Oklahoma State University, 2005, pp. 183-202.
3. Puckhaber, C. F., “Print-Registration Control in a Rotogravure Printing Press Combined with Extrusion-Coating or Lamination Processes,” Tappi Journal, Vol. 78, No. 3, 1995, pp. 144–154.
4. Puckhaber C. F., “Machine Direction Registration Problems Part 1,” Gravure, Spring 1996, pp. 26-32.
5. Puckhaber, C. F., “Machine Direction Registration Problems Part 2,” Gravure, Summer 1996, pp. 20-27.
6. Puckhaber, C. F., “Machine Direction Registration Problems Part 3,” Gravure, Fall 1996, pp. 18-23.
7. Weiss, H. W., “Improving Color Register on a Rotogravure Press,” Package Printing, April 1983, pp. 39, 67-69.
8. Brandenburg, G., “New Mathematical Models for Web Tension and Register Error,” Proceedings of the 3rd International IFAC Conference on Instrumentation and Automation in the Paper, Rubber and Plastic Industry, Vol. 1, May 1976, pp. 411-438.
9. Brandenburg, G., Geissenberger, S., Kink, C., Schall, N.-H., and Schramm, M., “Multimotor Electronic Line Shafts for Rotary Offset Printing Presses: A Revolution in Printing Machine Techniques,” IEEE/ASME Trans. Mechatronics, Vol. 4, Issue 1, March 1999, pp. 25-31.
10. Brandenburg, G., “Advanced Process Models and Control Strategies for Rotary Printing Presses,” Proceedings of the 11th International Conference on Web Handling, 2011.
11. Seshadri, A., Pagilla, P.R., and Lynch, J. E., “Modeling Print Registration in Roll-to-Roll Printing Presses,” Journal of Dynamic Systems, Measurement, and Control, Vol. 135, May 2013, pp. 031016-1.
12. Kang, H.-K., Lee, C.-W., and Shin, K.-H., “Compensation of Machine Directional Register in a Multi-Layer Roll-to-Roll Printed Electronics,” 2010 International Conference on Control Automation and Systems (ICCAS), 2010, pp. 2494-2497.
13. Walton, R. L., and Rice, B. S., “Web Longitudinal Dynamics,” Proceedings of the Fourth International Conference on Web Handling, Oklahoma State University, 1997, pp. 384-403.

14. Young, G. E. and Reid, K. N., "Lateral and Longitudinal Dynamic Behavior and Control of Moving Webs," Journal of Dynamics Systems, Measurement, and Control, Vol. 115, June 1993, pp. 309-317.
15. Young, G. E., Shelton, J. J. and Kardamilas, C., "Modeling and Control of Multiple Web Spans Using State Estimation," Journal of Dynamics Systems, Measurement, and Control, Vol. 111, No. 3, Sept. 1989, pp. 505-510.
16. Shin, K., "Distributed Control of Tension in Multi-Span Web Transport Systems," Ph.D. Thesis, Oklahoma State University, Stillwater, OK, 1991.
17. Ogata, K., Modern Control Engineering, 3rd ed., Prentice Hall, Englewood Cliffs, New Jersey, pp. 143-144, 1997.

APPENDIX - GOVERNING EQUATIONS

To derive the governing equations for longitudinal and registration dynamics, the following assumptions will be made: strain is uniform in a web span, web strain is much less than unity, no slip between web and roller, web is linearly elastic, web material properties are isotropic and homogeneous, web cross-sectional area is uniform, web thickness is small compared to the roller radii, and the web has only membrane stiffness.

Longitudinal Tension Dynamics

Figure 3 represents a simple three-span, two-roller conveyance path. The governing equation given for longitudinal tension dynamics was derived by Walton and Rice [13] and is shown below:

$$L_2 \cdot \frac{d}{dt}(\varepsilon_2) = \left(\frac{\dot{\theta}_2 R_2}{1 + \varepsilon_2} - \frac{\dot{\theta}_1 R_1}{1 + \varepsilon_1} \right) \cdot (1 + \varepsilon_2)^2. \quad \{10\}$$

The time rate of change of strain in span 2 is a function of span 1 and 2 strain, web velocity entering and exiting rollers, and the length of web in span 2.

Longitudinal Registration Dynamics

Consider the problem of registering patterns depicted in Figure 2 in the machine direction only. Assume that the patterns are printed with a pair of driven rotogravure coating rollers, as shown in Figure 3. On the first gravure roller, a "•" pattern is laid down. This pattern then conveys to a second gravure roller where the "+" pattern is laid down.

It is well known in the industry that steady-state registration between these patterns is only possible if $\dot{\theta}_1 = \dot{\theta}_2$ [3,8]. Thus, the change in steady-state registration for a relative change in the cylinders' angular orientation at steady state is:

$$\Delta X_{12}^{SS} = (\theta_1 - \theta_2) \cdot \left(\frac{R_1 + R_2}{2} \right). \quad \{11\}$$

A positive registration change means that more "•" than "+" are printed—"•" are "walking" forward with respect to the "+". Taking the time derivative of Equation {11} yields:

$$\frac{d}{dt}(X_{12}^{SS}) = \frac{\dot{\theta}_1 - \dot{\theta}_2}{2\pi} \cdot \frac{R_2 + R_1}{2} \cdot 2\pi = \left(\dot{\theta}_1 - \dot{\theta}_2 \right) \cdot \frac{R_2 + R_1}{2}. \quad \{12\}$$

There is a constant rate of registration error when $\dot{\theta}_1 \neq \dot{\theta}_2$. This equation only considers the steady-state registration; it ignores the effect of web stretch caused by tension transients on registration.

Again consider the problem of registering patterns depicted in Figure 2 in the machine direction only; however, this time we are interested in the effect of tension transients on registration. On the first gravure roller, a “•” pattern is laid down. This pattern then conveys to a second gravure roller. Assuming the surface velocities of the rollers are different, the web span between the two gravure rollers will stretch to a different strain than the incoming strain to the first gravure roller. The stretched web is now printed with the “+” pattern.

We assume web at nip 1 and nip 2 is printed at ε_1 and ε_2 , respectively (i.e., the strain of the web during printing is the strain of the web in the incoming span). Let x_1^0 and x_2^0 represent the length of a relaxed (untensioned) portion of pattern web printed at stations 1 and 2, respectively. Assuming no slip, the length of the tensioned patterned web printed at nip 1 per unit time is:

$$\dot{\theta}_1 R_1 \Delta t = x_1^0 (1 + \varepsilon_1). \quad \{13\}$$

Assuming no slip, the length of the tensioned patterned web printed at nip 2 per unit time is:

$$\dot{\theta}_2 R_2 \Delta t = x_2^0 (1 + \varepsilon_2). \quad \{14\}$$

Additionally, unchanging registration requires that the same length of untensioned web be conveyed through both nips ($x_1^0 = x_2^0$). If this is not true, a registration shift results. Thus, the difference in $x_2^0 - x_1^0$ represents the registration change (shift) in a time interval Δt .

$$\frac{x_2^0 - x_1^0}{\Delta t} = \frac{X_{21}^T}{\Delta t} = \left(\frac{\dot{\theta}_2 R_2}{1 + \varepsilon_2} - \frac{\dot{\theta}_1 R_1}{1 + \varepsilon_1} \right). \quad \{15\}$$

Letting Δt approach an infinitesimally small time yields the differential equation for the time rate of change for registration of an untensioned web:

$$\frac{d}{dt} (X_{21}^T) = \left(\frac{\dot{\theta}_2 R_2}{1 + \varepsilon_2} - \frac{\dot{\theta}_1 R_1}{1 + \varepsilon_1} \right). \quad \{16\}$$

The above equation represents the transient effects of tension dynamics on registration. It incorporates the effect of varying web strain on registration. Combining Eqs. (12) and (16) yields total time rate of change in registration error:

$$\frac{d}{dt} (X_{21}) = \frac{d}{dt} (X_{21}^T) + \frac{d}{dt} (X_{21}^{SS}) = \left(\frac{\dot{\theta}_2 R_2}{1 + \varepsilon_2} - \frac{\dot{\theta}_1 R_1}{1 + \varepsilon_1} \right) + \left(\dot{\theta}_1 - \dot{\theta}_2 \right) \cdot \frac{R_2 + R_1}{2}. \quad \{17\}$$

This expression may be integrated with respect to time to compute the total registration error in the untensioned web. The strains and angular velocities in Equation {17} represent two different points in time. The strain ε_2 is the strain in the web when it is printed at nip 2. The strain ε_1 represents the strain in the same piece of web when it was printed at nip 1. This happened approximately $\frac{L_2}{\theta_2 R_2}$ time units earlier. By the time the web arrives at nip 2, ε_1 and θ_1 have most likely changed. This transport delay will be depicted by a superscripted “delay”:

$$\frac{d}{dt}(X_{21}) = \left(\frac{\dot{\theta}_2 R_2}{1 + \varepsilon_2} - \frac{\dot{\theta}_1^{delay} R_1}{1 + \varepsilon_1^{delay}} \right) + \left(\dot{\theta}_1^{delay} - \dot{\theta}_2 \right) \cdot \frac{R_2 + R_1}{2}. \quad \{18\}$$

The steady-state strain for unvarying registration is obtained by setting the time rate of change in registration equal to zero and $\dot{\theta}_1 = \dot{\theta}_2$:

$$\varepsilon_2 = \frac{(1 + \varepsilon_1) \cdot R_2 - R_1}{R_1}. \quad \{19\}$$

Likewise, by setting the time rate of change of strain for web span 2 equal to zero in Equation {10} and $\dot{\theta}_1 = \dot{\theta}_2$, the same equation for steady-state ε_2 is obtained. (The superscripted “delay” is removed for steady state.) This result is satisfying in that both the tension and the registration equations yield the same result for ε_2 .

System Model of a Two-Station Printing Press with CR Registration Control

We now have equations to model longitudinal tension and registration dynamics. A simple web path of a two-station printing press with a compensator roller for registration control is shown in Figure 12. The basic equations to model the registration between stations 1 and 2, registration controls, web tensions, roller velocities, etc., are developed next.

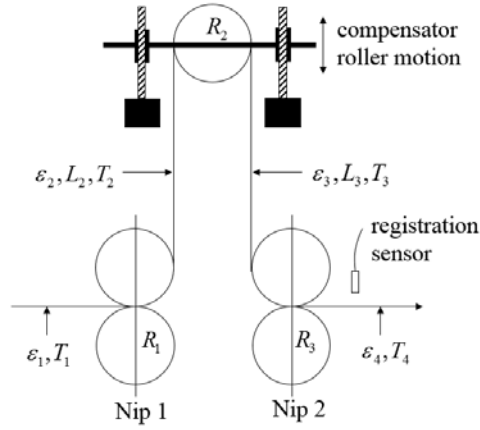


Figure 12 – Simple Two-Station Printing Press with Compensator Roller Registration Control

The acceleration of roller 2 is based on Newton's second law ($\dot{\theta}_1$ and $\dot{\theta}_3$ are inputs to model):

$$\frac{d}{dt}(\dot{\theta}_2) = \frac{T_3 - T_2}{J_2} \cdot R_2. \quad \{20\}$$

The web strain rates are based on Equation {10} (ε_1 and ε_2 are inputs to model):

Span 2:

$$\frac{d}{dt}(\varepsilon_2) = \frac{1}{L_2} \left(\frac{\dot{\theta}_2 R_2}{1 + \varepsilon_2} - \frac{\dot{\theta}_1 R_1}{1 + \varepsilon_1} \right) \cdot (1 + \varepsilon_2)^2 + \frac{V_{CR}}{L_2}. \quad \{21\}$$

Span 3:

$$\frac{d}{dt}(\varepsilon_3) = \frac{1}{L_3} \left(\frac{\dot{\theta}_3 R_3}{1 + \varepsilon_3} - \frac{\dot{\theta}_2 R_2}{1 + \varepsilon_2} \right) \cdot (1 + \varepsilon_3)^2 + \frac{V_{CR}}{L_3}. \quad \{22\}$$

The registration error between stations 1 and 2 is based on Equation {18}:

$$\frac{d}{dt}(X_{21}) = \left(\frac{\dot{\theta}_3 R_3}{1 + \varepsilon_3} - \frac{\dot{\theta}_1^{delay} R_1}{1 + \varepsilon_1^{delay}} + \left(\theta_1^{delay} - \dot{\theta}_3 \right) \cdot \frac{R_3 + R_1}{2} \right). \quad \{23\}$$

The vertical velocity V_{CR} of the compensator roller is based on active registration control:

$$V_{CR} = K_p (1 + \varepsilon_4) \cdot X_{21}. \quad \{24\}$$

The registration error X_{21} is for an unstretched piece of web. The factor $(1 + \varepsilon_4)$ accounts for the stretch in web span 4 where the registration sensor is located.

Web tensions are based on the following constitutive laws:

$$T_i = h_i w_i E_i \varepsilon_i = h \cdot w \cdot E \cdot \varepsilon_i, \quad \{25\}$$

Registration error of stretched web:

$$X_{21} = (1 + \varepsilon_4) \cdot \left(\int_0^t \frac{d}{d\tau} (X_{21}) \cdot d\tau + IC \right). \quad \{26\}$$

Compensator roller linear position (what controls steady-state registration):

$$X_{CR} = \int_0^t \frac{d}{d\tau} (V_{CR}) \cdot d\tau + IC. \quad \{27\}$$

System of a Two-Station Printing Press with DG Registration Control

If the compensator roller is “locked out” in the simple web path of a two-station printing press shown in Figure 12, we can use DG (advance or retard roller 3 with respect to roller 1) instead to control registration. The basic equations to model the registration between stations 1 and 2, registration controls, web tensions, roller velocities, etc., are basically the same as the compensator roller derivation, with these differences. First, the registration control loop, Equation {24}, is changed to:

$$V_{DG} = K_p (1 + \varepsilon_4) \cdot X_{21}. \quad \{28\}$$

Second, the angular velocities $\dot{\theta}_1$ and $\dot{\theta}_2$ are no longer equal, $\dot{\theta}_1 = \dot{\theta}^{ref}$ and $\dot{\theta}_3$ is given below:

$$\dot{\theta}_3 = \dot{\theta}^{ref} + \dot{\theta}_3^{trim} = \dot{\theta}^{ref} + V_{DG} \cdot \frac{2}{R_1 + R_3}. \quad \{29\}$$

Lastly, Equation {27} is changed to:

$$X_{DG} = \int_0^t \frac{d}{d\tau} (V_{DG}) \cdot d\tau + IC. \quad \{30\}$$

This represents advance or retard of the surface position between rollers 1 and 3 or:

$$(\theta_1 - \theta_3) \cdot \left(\frac{R_3 + R_1}{2} \right). \quad \{31\}$$

Numerical Simulation of a Tension Step with CR Control

In this section we will study the effect of a step in the input tension and a step in registration error on the performance of a simple two-station compensator roller-controlled printing press depicted in Figure 12. We will use ACSL™, a commercial ODE solver to model the examples in this section. We will use a second order Runge-Kutta numerical integration routine with a fixed time of 0.0001 s. In all examples, web

speed is 4.0 m/s, inlet tension T_1 is 100 N, web thickness is 4.5 μm , web width 1.6 m, Young's Modulus of the web is 4.7×10^6 kPa, web span lengths are 3 m, $R_1 = 0.25$ m, and R_3 is 25 μm larger. (Using Equations {19} and {25}, the effect of R_3 being 25 μm larger than R_1 on $T_3 - T_1$ is calculated to be 3.57 N. This is also seen in the example that follows.)

Using the equations developed in section A.3, we model the system response to a 20 N step in the inlet tension T_1 . Figure 13 shows a matrix of the results for three different proportional gains for the compensator registration loop. Columns 1, 2, and 3 show results for a proportional gain of 0.25, 1.0, and 2.0 inverse seconds, respectively. Rows 1, 2, and 3 show results for span 1 (dotted line) and span 3 (solid line) tensions, registration error, and compensator linear position, respectively.

Increasing registration gain from 0.25 to 1.0 to 2.0 results in a larger range and more oscillatory web tension, a similar range but more oscillatory registration error performance, and a larger range and more oscillatory compensator motion. Increasing the control gain much above 0.25 was not beneficial. A registration gain much larger than 2.0 results in slack tension and unstable behavior. The tension plots also show that $T_3 - T_1 = 3.57$ N as a result of R_3 radius being 25 μm larger than R_1 .

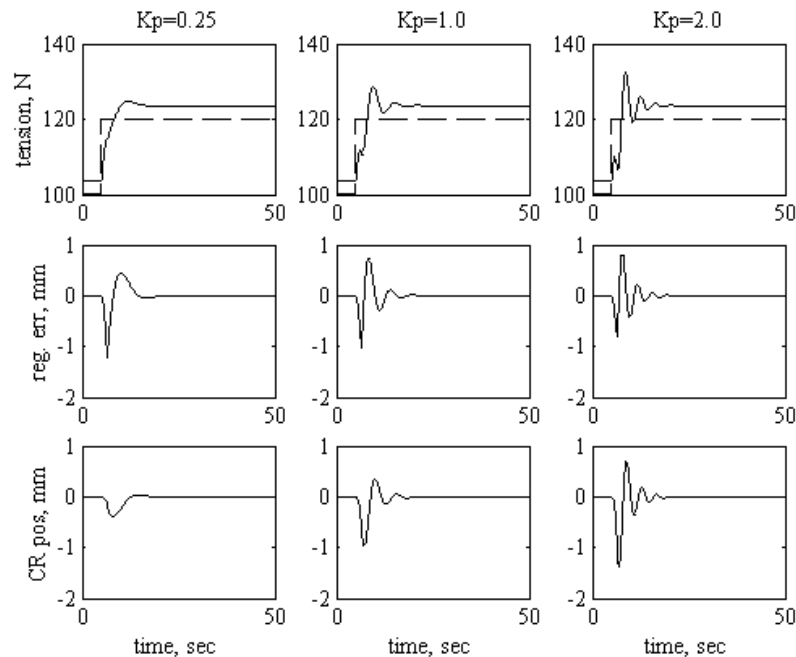


Figure 13 – Step of 20 N in Infeed Tension, Compensator Roller Control